Evaluation and optimization of the performance characteristics of fast response fiber optic oxygen gas probes

Jan Werner[ab]*, Mathias Belz[c], Karl-Friedrich Klein[bc], Tong Sun[a] and K.T.V. Grattan[a]

[a] *School of Mathematics, Computer Science and Engineering, City, University of London, Northampton Square, EC1V 0HB, London, U.K*

[b] *THM, University of Applied Science, Wilhelm-Leuschner-Strasse 13, 61169 Friedberg, Germany*

[c] *Lytegate GmbH, Ludwigstraße 36, 61169 Friedberg, Germany*

Abstract

Even though many different designs for currently available, fluorescence-based fiber optic sensors for measuring oxygen concentration (O_2) are well known (and indeed some are commercially available), they often are limited by their response time and long-term stability. This will cause problems in the important industrial applications of fiber optic sensors of this type that are developing, with limitations that are evident, for example, in physiology and other fields where *rapid* sensor responses are required. Research by a number of groups has discussed various new designs of fiber optical sensors, which have been developed in recent years where the key features of such probes to achieve the performance required are, for example, optimization of design features such as tip shape and coating layer thickness. The research reported in this paper represents an evaluation of such key factors to allow the design of better fiber optic-based sensors for oxygen measurement, where the optimized performance of a new, specially tapered tip O_2 sensor designed has been compared with the output of conventional and commercially available probe designs. The performance of a group of such sensors has been analyzed and cross-compared, examining the key features of such a probe including sensor accuracy, response time and overall long-term stability, as well as cross-sensitivity to any temperature changes which may occur in 'real' measurement situations.

Keywords: optical fiber sensors; O_2 measurement; oxygen sensing; fast response time; luminescence; fluorescence; microsensor; optical sensors; instrumentation; fiber optic; commercial; biomedical measurements.

* Corresponding author
E-mail address: jan.werner@iem.thm.de

1. Introduction

There is particular interest in detecting oxygen concentration (O_2) in a large field of applications today: the variety exemplified in, for example, the clinical analysis of blood [1], for quality control in the food and beverage industries [2] or even in seawater analysis [3]. As an example, McLeod *et al.* have used O_2 sensors to analyze the effects of ocean warming and associated changes in food supply for larval coral reef fish as part of a recent climate change study [4]. To obtain the data relevant for use with an eddy covariance correlation technique, small, fast response sensors are required to measure the O_2 changes over the sediment-water interfaces [5, 6], where the determination of O_2 concentration is a particularly important parameter. Further applications are evident across industry, especially in environmental monitoring and in biomedical research, and the field has been the subject of several review papers written in recent years e.g. [7].

Looking at conventional measurement techniques, the Clark electrode [8] is commonly used in industry for O_2 measurements: however, sensors of this type consume the analyte, and this issue can cause problems in some applications. Further, these sensors can experience interference from stray electromagnetic fields in certain industrial situations. Above all, they are fragile (they are made from thin glass) and often bulky, which requires them to be handled very carefully, especially for in-the-field use.

A highly effective alternative lies in the design of fiber optic sensors which are becoming more widely used in measurements like these since they do not consume the analyte (e.g. O_2), are reversible and importantly, given the small size of the fiber itself, are easy to miniaturize (< 50μm). Further, they can be employed in either the gas or the liquid phase, are inexpensive to produce in quantity and if there is electromagnetic interference present, they are unaffected by it [9]. The market for such optical fiber sensors is thus growing, and especially so for O_2 measurement. Looking at the way the situation has developed since 2000, more of these sensors have become commercially and are available for a wide range of commercial and industrial uses. Companies such as PyroScience GmbH (www.pyroscience.com), Ocean Insight Inc. (www.oceaninsight.com), PreSens Precision Sensing GmbH (www.presens.de), World Precision Instruments Inc.(www.wpiinc.com), Unisense (www.unisense.com) and Ohio Lumex (www.ohiolumex.com) now have a significant presence in the market; and research developments reported some years ago in the literature are now coming to fruition in commercially available devices. In that way, those who need sensors of this type can access many different system designs: they vary from the large (and thus robust) to very small (ideal for small sample volumes)[7].
Comparing and contrasting the techniques employed, absorbance, reflectance or luminescence-based techniques are amongst most widely used for O_2 sensing but the detection of luminescence intensity or decay time is a simple and easy to use route to a measurand-sensitive parameter (in comparison to ratiometric measurements, as only one type of indicator dye is needed). Some problems still can arise, unfortunately, due to photobleaching if high levels of incident radiation are used, or if not well designed resulting from interference from stray light and the drift of the electronic components used [10]. Such problems can be reduced or eliminated by better systems design, to eliminate such problems. Additionally, most fiber optic sensors of this type use an indicator dye immobilized in a supporting matrix, which typically is a polymer, attached to the sensor tip [11]. The sensor response time, drift and detection range (the key performance parameters) are influenced by the synergy of the effects on the sensor platform (here the fiber tip), the type of polymer and the indicator dye that have been used [12]. Therefore optimization of the sensor tip design is clearly important as a smaller tip can reduce the response time and this typically will mean a smaller amount of and thinner layer of coating, including the indicator, is present at the tip itself. In addition, the choice of optical fiber chosen will make a difference to the guidance of the light launched [13, 14].

Recognizing the importance discussed above for a fast response, over the years, a number of different luminescence-based O_2 sensors have been reported, with response times to O_2 changes (for ease of comparison here 90 % of saturation – Δt_{90}) ranging widely, from ~0.5 s to 100 s [15–19]. In previous work, a new and innovative tapered-tip design of a fiber optic O_2 sensor has already been intensively discussed [20, 21]. The O_2-sensitive coating used for this type of sensor consists of an indicator dye physically entrapped in a polymer matrix, which allows the physiologically important O_2 range (0 % to 20 %) to be covered. O_2 concentration changes are typically detected using the luminescence decay time changes (this being measured with a commercially available instrument) and having the advantage that changes in intensity (generated by the system) will not, in principle, affect the decay time measurement. The sensing system reported showed very fast responses to O_2 changes and a high long-term stability. This was achieved by increasing the effective area at the sensor tip, which allows optimization of the probe's light emission and the use of thinner layers. Furthermore, the sensor design reported has been successfully applied in a pH sensing approach [22, 23].

Building on the above, the work reported in this paper discusses the route towards making further progress in the design and implementation of such sensors and compares the highly advantageous properties of the O_2 sensors developed (e.g. fast response time and long-term stability) with those of conventional and commercially available probe designs. In addition, given that in the 'real world' the conditions under which such sensors are used are anything but ideal, the effects of external parameters such as temperature have also been investigated and results obtained discussed.

2. Theoretical background of O_2 quenching and widely used models

Photoluminescence, which underpins the operation of the sensor probe, is a well-known process that describes the emission of photons when a molecule is excited with light that is suitably absorbed and produces emission at specific wavelengths [7, 24]. The theoretical background is well set out elsewhere [7] but summarized here with reference to the key features of the probe design. Photoluminescence can be influenced by numerous processes – changes which are termed quenching – and represent a loss mechanism in the sensor scheme to be avoided. Thus for O_2-sensitive indicator dyes the presence of molecular O_2 reduces the luminescence intensity and the lifetime due to dynamic collision quenching of O_2 molecules in the excited electronic state S_1 (see Figure 1); and when returning back to ground state (S_0) no emission of a photon occurs. The process does not alter the molecules and is fully reversible [10, 24].

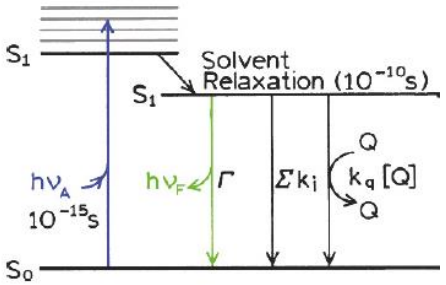

Figure 1: Modified Jablonski Diagram illustrating the process of collision quenching [24].

The Stern-Volmer equation is the well-known approach to describe this photophysical effect caused by collision quenching of O_2:

$$\frac{I_0}{I} = \frac{\tau_0}{\tau} = 1 + K_{SV}\,[O_2] \quad (1)$$

where τ_0 is the decay time and I_0 the luminescence intensity in absence of O_2. τ is the decay time and I the luminescence intensity in presence of O_2. K_{SV} is the Stern-Volmer constant and $[O_2]$ the concentration of O_2. However, recognizing that the Stern-Volmer equation only describes an ideal quenching system, many luminescent indicator dyes show non-linear behaviors. Thus two other popular models, Lehrer and Demas, are ideal to describe the effect of a quenchable and a non-quenchable site [7]:

Lehrer: $$\frac{I_0}{I} = \frac{\tau_0}{\tau} = \left(\frac{f}{1 + K_{SV}[O_2]} + (1 - f)\right)^{-1} \quad (2)$$

Demas: $$\frac{I_0}{I} = \frac{\tau_0}{\tau} = \left(\frac{f}{1 + K^1_{SV}[O_2]} + \frac{(1-f)}{1 + K^2_{SV}[O_2]}\right)^{-1} \quad (3)$$

where f and (1 − f) represent the relative contribution of each site to the total luminescence emission, K^1_{SV} and K^2_{SV} are the Stern–Volmer constants for the two sites while in the Lehrer model, the constant K^2_{SV} of the second site is assumed to be zero. The above provides a sufficient background to the subject for the discussion below – a wider discussion of the theoretical background to this work can be seen in the literature e.g. [7].

3. Material and Methods

3.1. Performance cross-comparison strategy

The approach is taken from the perspective of a user of a probe of the type discussed, seeking optimum performance for the application in view. When such a user is seeking to identify the most suitable probe for a particular application, a cross-comparison of a number of probe characteristics should be carried out and, in that way, the best choice *for that application* be made. Thus to highlight, analyze and cross-evaluate in a highly quantitative way the performance of a novel O_2 sensor design previously developed by the authors[20] (referred to as *Probe A1*), the performance of the probe has been compared with that of a conventional flat-tip design (referred to as *Probe A2*, see Figure 2 A), fabricated with the identical fiber type and coating material used with *Probe A1,* as well as with three commercially available O_2 probes.
To ensure breadth in this cross-comparison, two commercial probes (referred to as *Probe B* and *Probe C)* form a further part of that evaluation (see Figure 2 B&C). These are constructed, based on all-silica fibers with typical diameters of 100 µm/140 µm (core/cladding), the tips are coated with comparable O_2-sensitive layers, and these were used with a commercially available Microx TX3 device (purchased from Presens Precision Sensing GmbH). A further, third commercially available O_2 probe considered consists of an optical fiber with a core diameter of 1000 µm and protected in a stainless steel tube with an outer diameter of 1.587 mm (referred to as *Probe D*) was included in this cross-comparison. The probe tip is polished at an angle of about 45° and coated with an O_2-sensitive layer (see Figure 2 D). *Probe D* as well as the developed sensors (*Probe A1* and *Probe A2*) have been characterized with a neoFox instrument (purchased from Ocean Insight Inc.).

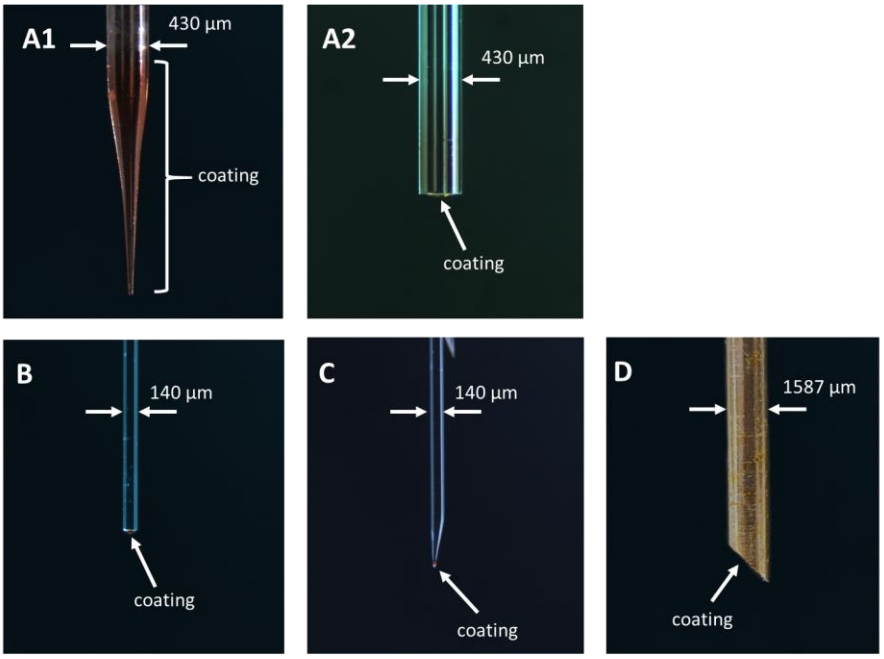

Figure 2: Images of the probes used for cross-comparison with the new sensor design showing the contrasting tip designs as well as the outer diameters and the coated areas. **A1**: New tapered tip design developed previously by the authors (*Probe A1*); **A2**: Developed flat design and used as reference (*Probe A2*); **B**: Flat commercial sensor (*Probe B*); **C**: Tapered commercial sensor (*Probe C*); **D**: Angled commercial sensor (*Probe D*).

3.2. Probe performance – approach taken in the cross-comparison

The range of different O_2 probes under study here have been calibrated using a temperature-regulated test chamber [20] and at different O_2 concentrations between 0 % and 20 % O_2 (changed in steps of 4 % O_2) set by two accurate and fast thermal mass flow meters/controllers for O_2 and N_2 gases (EL-FLOW Prestige, Bronkhorst LLC USA). To obtain the data reported, average values of the luminescence decay time were determined over a duration of 50 seconds, for each O_2 concentration considered, and fitted to the Lehrer model (Eq. 2). In this case, the Lehrer model requires the estimation of 3 key parameters (τ_0, K_{SV} and f), to fit the calibration data, representing the luminescence response versus the O_2 concentration. To undertake the calibration and determine the response time, each sensor was placed in the temperature regulated chamber ($T_{const.}$ = 25°C). In the tests, first, pure nitrogen (0 % O_2) was passed through the chamber for about 80 seconds, then the gas mixture was changed quickly to 20 % O_2. After a further ~ 180 s, the gas mix was changed rapidly to pure nitrogen (0 % O_2) back again. Using the data collected with each instrument, the rise and fall times representing the sensor response were then determined at Δt_{90} (90 % of saturation).
Such probes need to work well in different temperature regimes and so the effect of temperature on the fiber optic O_2 probes was investigated (emphasizing the physiological important range between 25°C and 40°). To do so, each sensor was placed in the temperature regulated chamber after which the temperature was set to 25°C and concentrations of 0 %, 4 %, 8 %, 12 %, 16 % and 20 % O_2 were passed through the chamber for about 30 s in each case. This procedure was systematically repeated over a number of temperatures, increasing the temperatures, in steps of 5°C, until the maximum value (of 40°C) was reached. For each temperature and O_2 concentration, the luminescence decay time (obtained from the sensor tip) was determined by averaging the measured signals over a time interval of about 10 s.

Finally, good long-term stability is critical for success and this aspect was studied. This was done for *Probe A1* and compared with a commercially available tapered tip O_2 probe (*Probe C*) – investigated during continuous irradiation (with light pulses generated every 0.5 s) and for maximum duration of 16 days (*Probe A1* only). To analyze the effect of photobleaching (and thus the sensor drift) of both probe designs, calibration curves (decay time & intensity values) were measured every second day when using *Probe C* and every fourth day when using *Probe A1*.

4. Experimental results and discussion

This experimental section shows the results of the cross-comparison carried out: examining the performance of the novel O_2 probe design and comparing this with the commercially available and conventional O_2 probes mentioned above. To do so, the data collected are discussed and key performance aspects compared in respect of (i) probe calibration curves, (ii) signal strengths (and thus noise in the signal), (iii) response times and (iv) temperature 'cross-talk' issues.

Figure 3 shows the calibration data obtained from the five different probe designs that are discussed. These are described, as summarized in Table 1.

Table 1: Summary of the different probes evaluated and cross-compared in this study.

Sensor	Description
Probe A1	novel O_2 sensor design based on an optimized tapered tip and developed previously by the authors [20]
Probe A2	conventional flat-tip O_2 sensor developed by the authors and used for a direct comparison of sensor performance
Probe B	commercially available flat-tip O_2 sensor
Probe C	commercially available O_2 sensor with a conventional tapered tip
Probe D	commercially available O_2 sensor with an angled tip

4.1. Comparison of calibration data and signal strength of O_2 probes

For comparison, the calibration curves are plotted to show the ratio τ_0/τ versus O_2, where τ_0 is the decay time in the absence of O_2 and τ the decay time in the presence of O_2.

The sensitivity of an O_2 probe can be characterized by the Stern-Volmer constant K_{SV} [25] and this has been estimated for the O_2 sensors by fitting the Lehrer model (applying Eq. 2). As shown in Table 2, this model describes the experimental results of all sensors with a very high level of precision (R^2: 0.9999). Due to the similar coating material used, the sensor probes (*Probe A1* and *Probe A2*) developed by the authors previously show almost identical calibration curves (see Figure 3 blue and green curves) and comparable K_{SV} values of approximately 0.13 (see Table 2). In comparison to *Probe B* and *Probe C*, these commercially available probes have a slightly higher sensitivity to O_2. However, the reasonable assumption is made that these two commercial probes have a comparable O_2-sensitive material (polymer and indicator) applied to the probe tips as used in the developed sensors (*Probe A1* and *Probe A2*), but with a slightly different

formulation, resulting in the small variations in O_2 sensitivity. In general, the choice of polymer host and indicator dye as the sensing element plays a critical role in the overall performance of the sensor, and as well the permeability of a polymer to O_2 is an additional factor, influencing the K_{SV} parameter significantly [25]. This effect is reflected in the calibration data obtained with commercial *Probe D*. With a K_{SV} value of 0.03, this fiber optic O_2 sensor has the lowest sensitivity to O_2 for the range investigated, mainly due to another polymer, a hydrophobic sol-gel matrix, used as host material for the indicator dye.

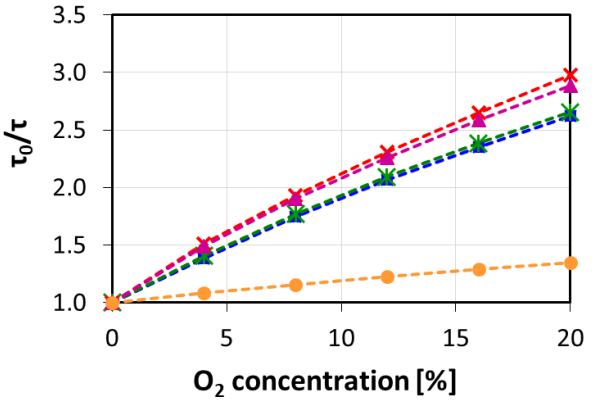

Figure 3: Calibration curves showing the ratio τ_0/τ versus O_2 of the five different probe designs. Green: *Probe A1*, blue: *Probe A2*, red: *Probe B*, violet: *Probe C*, orange: *Probe D*.

Table 2: Estimated parameters (τ_0, K_{SV} and f) of the fitted Lehrer model and correlation coefficient R^2 determined for the five different O_2 probes investigated.

Sensor	τ_0 [µs]	K_{SV}	f	K (= K_{SV}*f)	R^2
Probe A1	42.3	0.130	0.867	0.113	0.9999
Probe A2	42.2	0.129	0.866	0.109	0.9999
Probe B	50.1	0.146	0.888	0.130	0.9999
Probe C	52.1	0.132	0.892	0.118	0.9999
Probe D	2.9	0.033	0.653	0.021	0.9999

To compare the signal strengths of each probe, the emission intensities have been normalized using the following equation:

$$I_{norm.} = \frac{I_M}{I_{Max}} \quad (4)$$

where I_M (unit: counts - cts) is the measured O_2-dependent luminescence intensity obtained with the neoFox or Microx TX3 instrument and I_{MAX} the maximum intensity values (here: 65535 cts) of both instrument.

Comparing the O_2-dependent emission intensities of the three probes used with the neoFox instrument (see Figure 4, left), the sensor *Probe A1* not only shows the highest signal strength around 0 % O_2 (the initial point where no O_2 is present), it also has the greatest dynamic range, with a positive effect on the signal-to-

noise ratio as well as the long-term stability of the sensor. As an example, the excitation intensity can be reduced which increases the lifetime of the sensor and reduces the signal drift related to the photobleaching, without significantly affecting the signal quality (noise). As can be clearly seen, the commercially available sensor (*Probe D*, orange curve) has sufficient emission intensities in the mid-range of the instruments' detection range, while the reference *Probe A2* shows the lowest signal strength of all sensor concepts investigated with the neoFox instrument – this is not a very efficient probe design, especially when compared with the optimized tapered probe design (*Probe A1*). Furthermore, this has also been observed for *Probe B* and *Probe C* used with the Microx TX3 instrument (see Figure 4, right). Here, the tapered-tip sensor (*Probe C*, violet curve) shows increased emission intensities compared to the flat-tip probe design (*Probe B*, red curve), and thus highlights the advantage of a tapered-tip sensor design on the signal strength in general.

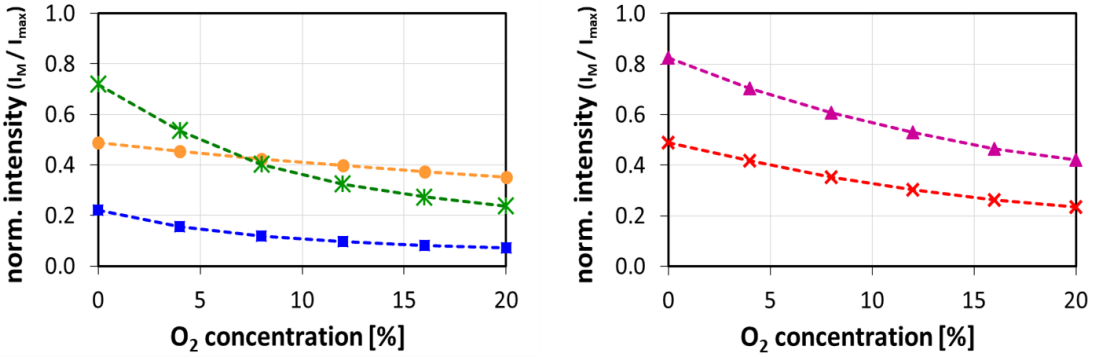

Figure 4: Curves showing the normalized amplitude (I_M/I_{Max}) versus O_2 of the five different probe designs.
Left: Results obtained using the neoFox device and *Probe A1* (green), *Probe A2* (blue) as well as commercial sensor *Probe D* (orange). Right: Results obtained using the Microx TX3 instrument and two commercial sensors *Probe B* (red) and *Probe C* (violet).

4.2. Comparison of response time of O_2 probes

Figure 5 shows the response curves of the five calibrated O_2 probe designs and Table 3 the rise time ($\Delta t_{90,rise}$) and fall time ($\Delta t_{90,fall}$) determined for each sensor (see Figure 5A2).

The results obtained clearly show that the most recently developed tip design (*Probe A1*) has the fastest response to O_2 changes (see Figure 5A1). With a rise time of ~ 0.3 s and a fall time of ~ 0.2 s, *Probe A1* is even significantly faster than the commercially available probes used as reference here. The comparison between *Probe A2* (see Figure 5A2) and *Probe A1* (see Figure 5A1) shows not only a significant improvement in response time, but also a better signal-to-noise ratio with this new tip design. However, the response time of *Probe A2* is negatively influenced by a relative thick coating required, to obtain a sufficient emission signal strength.

Due to a smaller amount of coating and the thinner layer used, the commercially available sensor with a tapered tip (*Probe C,* Figure 5C) already is seen to show faster response times to O_2 changes, compared to commercial *Probe B* (see Figure 5B) and this thus indicates the positive effect of a tapered tip on the sensor

performance. However, with a rise time of ~ 2.0 s and a fall time of ~ 1.6 s the response to O_2 is still a factor of about 6.6 slower than the innovative probe design developed by the authors.
Although *Probe D* is a relatively large sensor, the thin layer coated on the angled tip and the coating composition used, have a positive effect on the response time ($\Delta t_{90,rise}$ = 11,4 s and $\Delta t_{90,fall}$ = 7.4 s). However, a disadvantage of this commercial O_2 sensor is that it requires an additional time of 70 s to reach steady-state and shows an inaccuracy of ~ 0.8 % O_2 at 20 % O_2 (see Figure 5D), an effect not seen for the other probe designs.

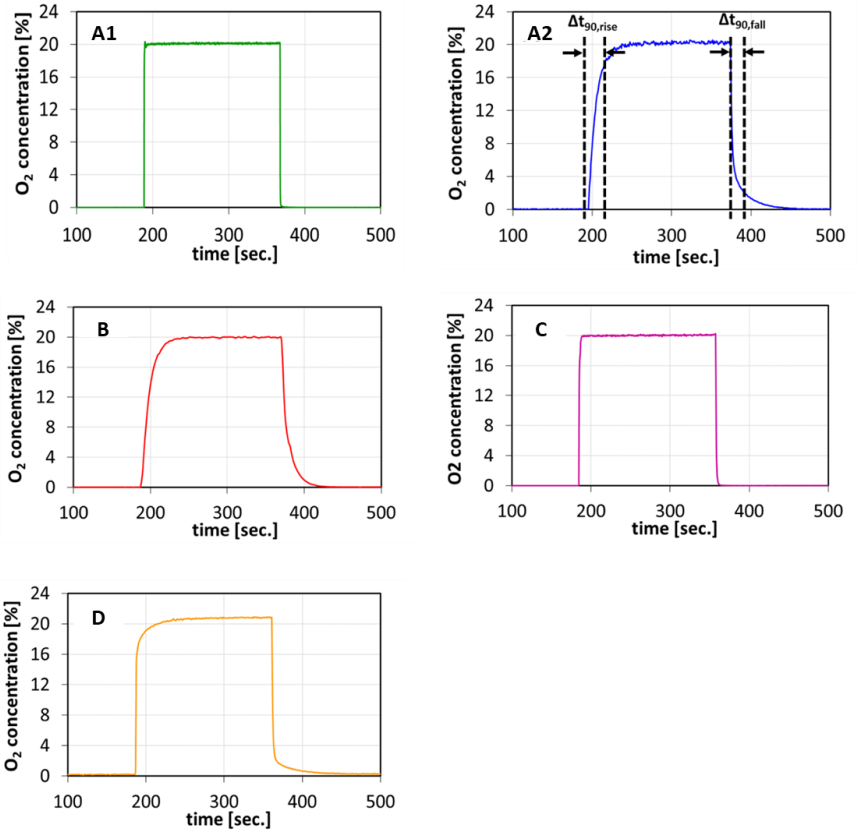

Figure 5: Measured response time curves of the five different probe designs due to a rapid change from 0 % to 20 % O_2 and back to 0 % O_2 again. Rise times determined at $\Delta t_{90,rise}$ and fall times at $\Delta t_{90,fall}$ (exemplary shown in A). **A1**: response time of *Probe A1,* **A2**: response time of reference *Probe A2*, **B:** response time of *Probe B*, **C**: response time of *Probe C*, **D**: response time of *Probe D*.

Table 3: Rise ($\Delta t_{90,rise}$) and fall times ($\Delta t_{90,fall}$) determined for the five different probe designs investigated.

Sensor	$\Delta t_{90,rise}$ [s]	$\Delta t_{90,fall}$ [s]
Probe A1	0.3	0.2
Probe A2	23.3	17.6
Probe B	26.0	21.2
Probe C	2.0	1.6
Probe D	6.5	6.4

4.3. Comparison of temperature effects on the O_2 probes studied

The effect of temperature changes causes one of the largest sources of error in optical O_2 sensors, since the luminescence of all such indicators shows a *cross-sensitivity* to thermal quenching. However, temperature changes also exert complex multiple influences on O_2-sensitive indicators, such as the fluorescence quantum yield, the decay time and the quenching constant. Further, the cross-sensitivity to temperature does not only depend on the indicator itself as it additionally significantly influences the solubility and the diffusion of O_2 in the supporting materials (e.g. polymers) used [10]. Thus, only relatively few studies on the temperature dependence of optical O_2-sensitive materials are available and usually only one (or a few) of the effects mentioned above is described. However, the temperature effects on the decay time of the newly developed tapered tip design (*Probe A1*) have already been discussed in detail and for a series of sensors in the literature [20].

To compare the results of the different probe designs used in this research, the absolute O_2 errors (% O_2) are shown in Figure 6. In general, all five probes show a linear temperature-induced drift of the luminescence decay time, since the luminescence decay times of such indicator dyes shorten with increasing temperature values. This effect is well known and has been used very effectively in stand-alone temperature sensors [26]. As can be seen, the changes in decay time lead to increasing absolute O_2 errors at increasing temperatures over the temperature range studied, and are additionally dependent on the O_2 concentration.

Looking more closely at the results obtained, the newly developed O_2 sensor (*Probe A1*, Figure 6A1) shows an optimized temperature stability and the lowest absolute O_2 error of < 3 % O_2 (determined at maximum values of 40°C and 20 % O_2) compared to the other O_2 probes (with maximum values between 4 % and 5 % O_2). Furthermore it indicates, that the temperature cross-talk of such sensors depends not only on the materials used (indicator dye and polymer), but also on the construction of the probe tip itself and the amount of coating material applied. This is also evident when comparing the flat-tip probe (*Probe A2*, Figure 6A2) with the new tapered-tip probe (*Probe A1*, Figure 6B). Both sensors were made from the same type of glass fiber and coated with an identical O_2-sensitive layer, but *Probe A2* has an increased O_2 error over the entire range investigated. Since there are only few reports in the literature of the temperature dependence of luminescence-based materials in combination with probe design, and the currently available results cannot describe the increased resistance to temperature interference, further work is needed to investigate the parameters that influence this behavior. This we plan to undertake and report in the future.

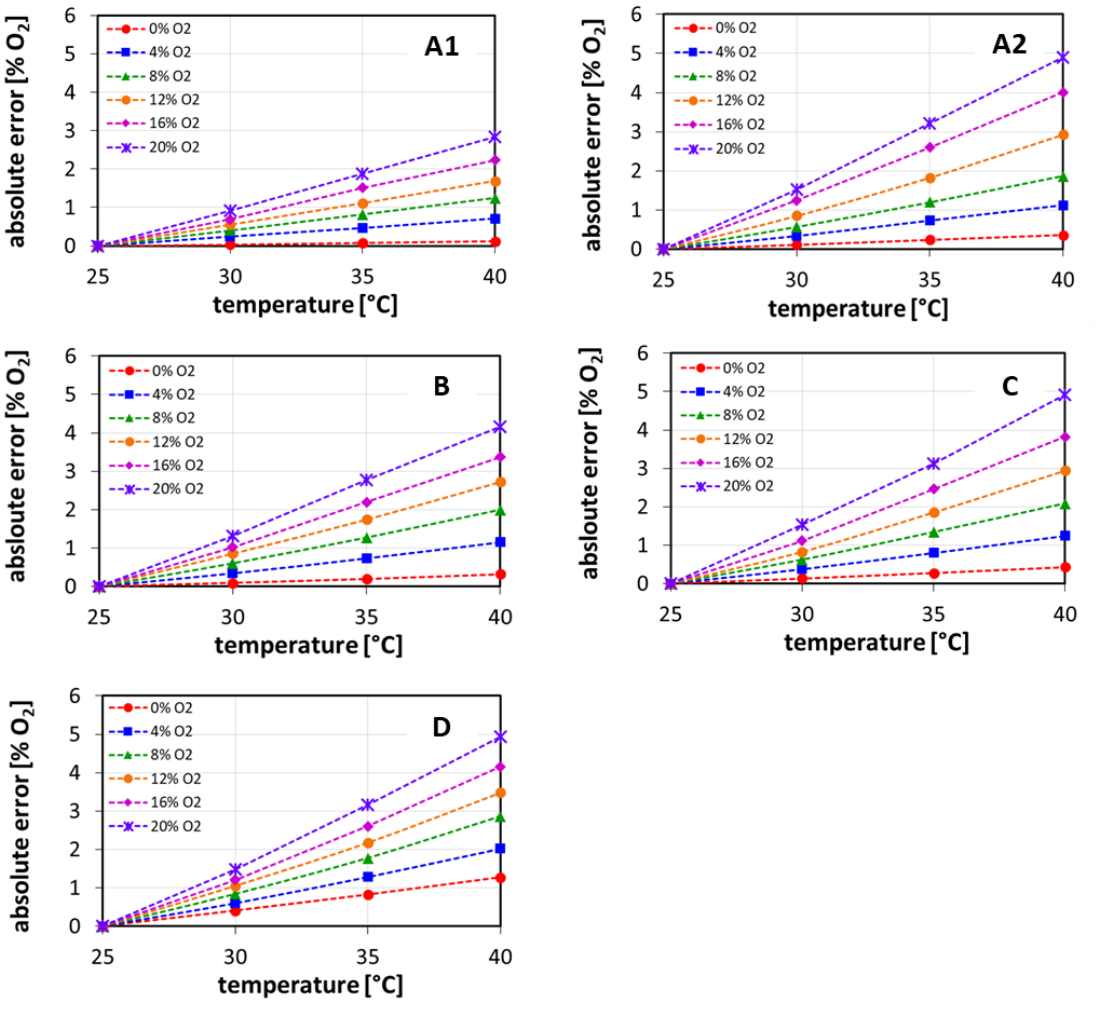

Figure 6: Effect of temperature on the five different probe designs showing the absolute O_2 error (% O_2) over temperature (between 25°C and 40°C) and determined for O_2 concentrations between 0 % and 20 % O_2.
A1: temperature response of *Probe A1,* **A2**: temperature response of reference *Probe A2*, **B:** temperature response of *Probe B*, **C**: temperature response of *Probe C*, **D**: temperature response of *Probe D*.

4.4. Comparison of long-term stability of the O_2 probes studied

Long-term stability of probes is particularly important, including to have a long 'shelf life' to give a positive sales advantage. To investigate and compare the long-term stability of the improved tapered-tip probe (*Probe A1*) with a commercially available and conventional tapered-tip probe (*Probe C*), Figure 7 and Figure 8 show the results obtained in a long-term experiment (of a maximum of 16 days duration). In addition, this experiment compared the use of two measurement systems, as *Probe C* was used with the Microx TX3 instrument and *Probe A1* was used with the neoFox device. Figure 7 shows the determined calibration curves with decay time versus O_2 concentration and Figure 8 shows the calibration curves with amplitude (emission intensity) versus O_2 concentration.

As seen from the results, the total emission intensity of *Probe C* decreases significantly after two days of use (see Figure 8, left) and already reaches the detection limit of the Microx TX3 instrument. Comparing the intensity values measured on the second day with the reference intensity values obtained at the beginning of the experiment (day 0), the average signal strength decreased by about 88 %. The relatively high photobleaching rate is mainly influenced by the very small amount of O_2-sensitive coating on the tapered tip and also leads to a significant shift in the measured decay times (see figure 7, left). With a relative decay time decrease of about 22 %, a re-calibration would be necessary after a maximum duration of 2 days continues use, which corresponds to 365,600 measuring points.

In comparison, *Probe A1* exhibits a significantly increased long-term stability and thus an exceptional sensor lifetime. The long-term stability and response time are positively affected by the narrow profile tip design, which allows very thin coatings and yet detection of luminescence signals over a large effective area of the tip, allowing much faster diffusion of O_2 and increased long-term stability. Even after 16 days of continuous irradiation, no significant shift in the decay time could be observed (see Figure 7, right). With a very low relative drift of about 0.04 %/day, the decay time has been seen to be very stable. Thus and where a reasonable measurement error of ≈ 0.1 % O_2 (for O_2 concentrations < 20 % O_2) is acceptable, a re-calibration of the sensor would then be required after 2,193,600 measuring points or 12 days of a continuous use – which is much longer than is needed for many biomedical or even industrial applications. In addition, the improved long-term stability is also reflected in the emission intensity curves measured and shown in Figure 8 (right). As expected and due to photobleaching, the calibration curves shift to lower intensity values, but with a relative drift in signal strength of about 0.95 %/day, the developed probe design shows a particularly favorable photostability and sensor lifetime for many applications.

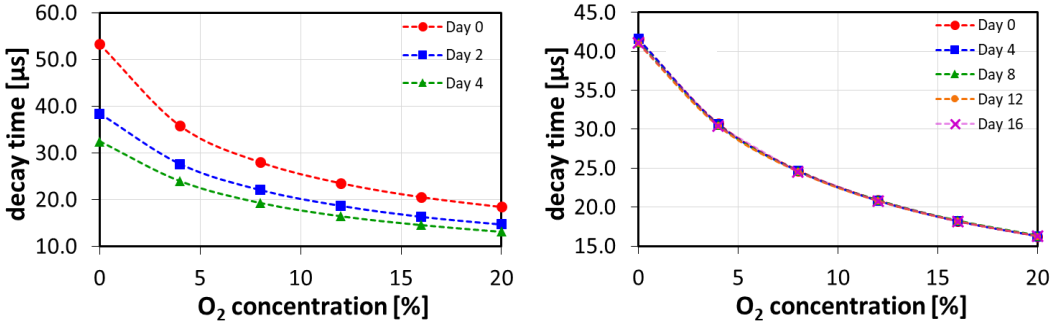

Figure 7: Calibration curves (decay time versus O_2 concentration) of *Probe C* (left) and the new tapered-tip sensor *Probe A1* (right) during a long-term experiment. *Probe C* was continuously irradiated for 4 days and *Probe A1* was continuously irradiated for 16 days.

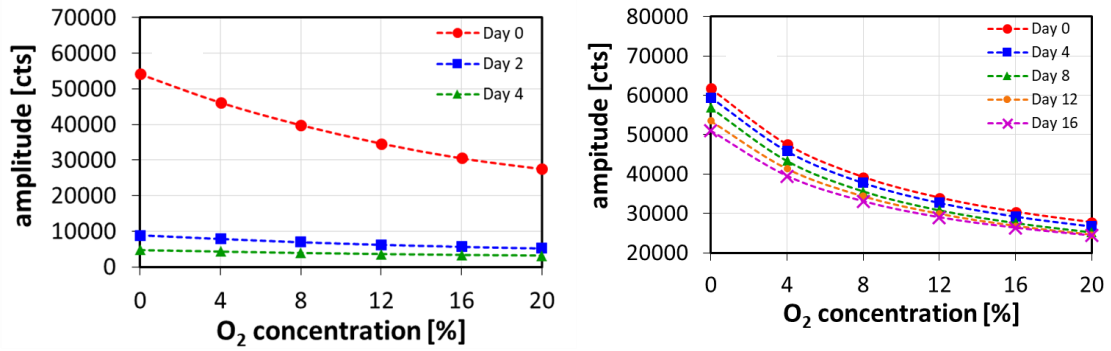

Figure 8: Calibration curves (emission amplitude versus O_2 concentration) of *Probe C* (left) and the new tapered-tip sensor *Probe A1* (right) during a long-term experiment. *Probe C* was continuously irradiated for 4 days and *Probe A1* was continuously irradiated for 16 days.

5. Conclusions

The paper has been focused on a comprehensive discussion of recently developed and performance-optimized fiber optic O_2 probes and a cross-comparison with the performance of several commercially available probes. The results reported reflect an extensive investigation of important parameters that remain highly promising. In this investigation, the results indicate that *Probe A1* shows a significant improvement in sensor performance when compared to conventional and commercially available probe designs and systems. All the sensors investigated have been calibrated with a very high level of precision (R^2: 0.9999) using two commercially available luminescence decay time measurement instruments.

The key feature of the new probe developed by the authors is that the sensor shows extremely fast response times to O_2 changes of $\Delta t_{90,rise} \approx 0.3$ s (increasing O_2 from 0 % to 20 %) and $\Delta t_{90,fall} \approx 0.2$ s (decreasing O_2 from 20 % to 0 %). As has been shown, this is significantly faster (a factor 6.6) than a conventional tapered-tip O_2 probe used as reference in this work. In combination with the commercial signal processing unit used, the recently developed O_2 probe has been shown to be very stable in a study carried out over a very long period of time. In comparison with a commercially available tapered probe, the sensor exhibits exceptional long-term stability during an experiment with 16 days of continuous irradiation. With a very low relative drift of about 0.04 %/day, the measured decay time has been seen to be very stable, thereby reducing the need for re-calibration significantly. A potential user only would need to re-calibrate the sensor after a long period of time (after 12 days compared to 2 days when using a conventional O_2 probe design) – ideal for commercial uses of such sensors.

Furthermore, the important temperature 'cross-talk' was investigated in the physiologically relevant temperature range (between 25°C and 40°C) and compared across the available O_2 probes. The results obtained show an improved temperature stability of the sensor design itself and, most importantly, a linear relationship between temperature and decay time. When highly accurate measurements of O_2 concentration between 25°C and 40°C are required, this allows a relative simple temperature compensation. A technique that can be applied is using a small length of rare-earth doped fiber whose decay time will also change with temperature, but is unaffected by O_2 concentration changes, or to include a Fiber Bragg Grating or a Long Period Grating temperature sensor.

Acknowledgements

The authors wish to thank World Precision Instruments Germany GmbH, Friedberg (Hessen), for the financial support. Kenneth Grattan and Tong Sun acknowledge support from the Royal Academy of Engineering.

References

[1] S. Kojima and H. Suzuki, "A Micro Sensing System for Blood Gas Analysis Constructed With Stacked Modules," *IEEJ Trans. SM*, vol. 124, no. 4, pp. 111–116, 2004, doi: 10.1541/ieejsmas.124.111.

[2] D. B. Papkovsky, N. Papkovskaia, A. Smyth, J. Kerry, and V. I. Ogurtsov, "Phosphorescent Sensor Approach for Non-Destructive Measurement of Oxygen in Packaged Foods: Optimisation of Disposable Oxygen Sensors and their Characterization Over a Wide Temperature Range," *Analytical Letters*, vol. 33, no. 9, pp. 1755–1777, 2000, doi: 10.1080/00032710008543157.

[3] J. F. Gouin, F. Baros, D. Birot, and J. C. André, "A fibre-optic oxygen sensor for oceanography," *Sensors and Actuators B: Chemical*, vol. 39, 1-3, pp. 401–406, 1997, doi: 10.1016/S0925-4005(97)80242-0.

[4] I. M. McLeod *et al.*, "Climate change and the performance of larval coral reef fishes: the interaction between temperature and food availability," *Conservation physiology*, vol. 1, no. 1, cot024, 2013, doi: 10.1093/conphys/cot024.

[5] L. Chipman *et al.*, "Oxygen optodes as fast sensors for eddy correlation measurements in aquatic systems," *Limnol. Oceanogr. Methods*, vol. 10, no. 5, pp. 304–316, 2012, doi: 10.4319/lom.2012.10.304.

[6] P. Berg and M. Huettel, "Monitoring the Seafloor Using the Noninvasive Eddy Correlation Technique: Integrated Benthic Exchange Dynamics," *Oceanography*, vol. 21, no. 4, pp. 164–167, 2008. [Online]. Available: www.jstor.org/stable/24860020

[7] J. Werner, M. Belz, K.-F. Klein, T. Sun, and K.T.V. Grattan, "Fiber optic sensor designs and luminescence-based methods for the detection of oxygen and pH measurement," *Measurement*, vol. 178, p. 109323, 2021, doi: 10.1016/j.measurement.2021.109323.

[8] L. C. CLARK, R. WOLF, D. GRANGER, and Z. TAYLOR, "Continuous recording of blood oxygen tensions by polarography," *Journal of applied physiology*, vol. 6, no. 3, pp. 189–193, 1953, doi: 10.1152/jappl.1953.6.3.189.

[9] X.-d. Wang and O. S. Wolfbeis, "Fiber-optic chemical sensors and biosensors (2008-2012)," *Analytical chemistry*, vol. 85, no. 2, pp. 487–508, 2013, doi: 10.1021/ac303159b.

[10] X.-d. Wang and O. S. Wolfbeis, "Optical methods for sensing and imaging oxygen: materials, spectroscopies and applications," *Chemical Society reviews*, vol. 43, no. 10, pp. 3666–3761, 2014, doi: 10.1039/C4CS00039K.

[11] I. Klimant, V. Meyer, and M. Kühl, "Fiber-optic oxygen microsensors, a new tool in aquatic biology," *Limnol. Oceanogr.*, vol. 40, no. 6, pp. 1159–1165, 1995, doi: 10.4319/lo.1995.40.6.1159.

[12] C. McDonagh, C. S. Burke, and B. D. MacCraith, "Optical chemical sensors," *Chemical reviews*, vol. 108, no. 2, pp. 400–422, 2008, doi: 10.1021/cr068102g.

[13] K.-F. Klein, C.P. Gonschior, X.Ruan, M.Bloos, G.Hillrichs, H.Poisel, "Transmission of skew modes in polymer- and silica-based step-index fibers," *Proc. 18th POF-conference*, no. 45, 2009.

[14] Arne Wilhelm Zimmer, Philipp Raithel, Mathias Belz, Karl-Friedrich Klein, "Analysis of spectral light guidance in specialty fibers," *in Proc. SPIE 9886-34*, 2016.

[15] C.-S. Chu and Y.-L. Lo, "High-performance fiber-optic oxygen sensors based on fluorinated xerogels doped with Pt(II) complexes," *Sensors and Actuators B: Chemical*, vol. 124, no. 2, pp. 376–382, 2007, doi: 10.1016/j.snb.2006.12.049.

[16] G. Holst, R. N. Glud, M. Kühl, and I. Klimant, “A microoptode array for fine-scale measurement of oxygen distribution,” *Sensors and Actuators B: Chemical*, vol. 38, 1-3, pp. 122–129, 1997, doi: 10.1016/S0925-4005(97)80181-5.

[17] S.-K. Lee and I. Okura, “Optical Sensor for Oxygen Using a Porphyrin-doped Sol–Gel Glass,” *Analyst*, vol. 122, no. 1, pp. 81–84, 1997, doi: 10.1039/A604885D.

[18] S.-K. Lee and I. Okura, “Photoluminescent determination of oxygen using metalloporphyrin-polymer sensing systems,” *Spectrochimica Acta Part A: Molecular and Biomolecular Spectroscopy*, vol. 54, no. 1, pp. 91–100, 1998, doi: 10.1016/S1386-1425(97)00206-0.

[19] G. R. McDowell, A. S. Holmes-Smith, M. Uttamlal, C. Mitchell, and P. H. Shannon, “A robust and reliable optical trace oxygen sensor,” *SPIE, Optical Sensors*, Vol. 10231, 2017, doi: 10.1117/12.2265561.

[20] J. Werner, M. Belz, K.-F. Klein, T. Sun, and K.T.V. Grattan, “Design and comprehensive characterization of novel fiber-optic sensor systems using fast-response luminescence-based O2 probes,” *Measurement*, p. 110670, 2021, doi: 10.1016/j.measurement.2021.110670.

[21] J. Werner, M. Belz, K.-F. Klein, T. Sun, and K.T.V. Grattan, “Fast response time fiber optical pH and oxygen sensors,” in *Optical Fibers and Sensors for Medical Diagnostics and Treatment Applications XX*, San Francisco, United States, Feb. 2020 - Feb. 2020, p. 56. [Online]. Available: https://www.spiedigitallibrary.org/conference-proceedings-of-spie/11233/2566993/Fast-response-time-fiber-optical-pH-and-oxygen-sensors/10.1117/12.2566993.full

[22] J. Werner, M. Belz, K.-F. Klein, T. Sun, and K. T. V. Grattan, “Characterization of a fast response fiber-optic pH sensor and illustration in a biological application,” *Analyst*, vol. 146, no. 15, pp. 4811–4821, 2021, doi: 10.1039/D1AN00631B.

[23] J. Werner, M. Belz, K.-F. Klein, T. Sun, and K. Grattan, “Characterization of a fast response fiber-optic pH sensor and measurements in a biological application,” in *Optical Fibers and Sensors for Medical Diagnostics, Treatment and Environmental Applications XXI*, Online Only, United States, Mar. 2021 - Mar. 2021, p. 6. [Online]. Available: https://www.spiedigitallibrary.org/conference-proceedings-of-spie/11635/2585735/Characterization-of-a-fast-response-fiber-optic-pH-sensor-and/10.1117/12.2585735.full

[24] J. R. Lakowicz, Ed., *Principles of Fluorescence Spectroscopy*. Boston, MA: Springer US, 2006.

[25] A. Apostolidis, “Combinatorial approach for development of optical gas sensors - concept and application of high-throughput experimentation,” Universität Regensburg, 2005.

[26] T. Sun, Z. Y. Zhang, K. T. V. Grattan, and A. W. Palmer, “Ytterbium-based fluorescence decay time fiber optic temperature sensor systems,” *Review of Scientific Instruments*, vol. 69, no. 12, pp. 4179–4185, 1998, doi: 10.1063/1.1149267.